

Impact of long-range transport over the Atlantic Ocean on Saharan dust optical and microphysical properties based on AERONET data

Cristian Velasco-Merino¹, David Mateos¹, Carlos Toledano^{1*}, Joseph M. Prospero², Jack Molinie³,
Lovely Euphrasie-Clotilde³, Ramiro González¹, Victoria E. Cachorro¹, Abel Calle¹, Angel M. de
5 Frutos¹

¹Grupo de Óptica Atmosférica, Dpto. de Física Teórica Atómica y Óptica, Universidad de Valladolid, Spain

²Cooperative Institute for Marine and Atmospheric Studies, Rosentiel School of Marine and Atmospheric Science,
University of Miami, Miami, Florida, USA

³Laboratory of Geosciences and Energy, Université des Antilles, Guadeloupe

10 *Correspondence to:* C. Toledano (toledano@goa.uva.es) Office B110, Grupo de Óptica Atmosférica, Dpto. de Física Teórica
Atómica y Óptica, Fac. Ciencias – UVa, Paseo Belén 7, CP 47011, Valladolid.

Abstract. Arid regions are a major source of mineral dust aerosol. Transport from these sources can have a great impact on
aerosol climatology in distant regions. In order to assess the impact of dust on climate we must understand how dust
properties change after long distance transport from sources. This study addresses the changes in columnar aerosol properties
15 when mineral dust outbreaks from West Africa arrive over the eastern Caribbean after transport across the Atlantic Ocean, a
transit of 5 – 7 days. We use data from the NASA Aerosol Robotic Network (AERONET) located at five Caribbean and two
West African sites to characterize changes in columnar aerosol properties: aerosol optical depth (AOD), size distribution,
single scattering albedo, and refractive indexes. We first characterized the local aerosol climatology at each site and then
using air mass back trajectories we identified those days when trajectories over Caribbean sites back-tracked to West
20 Africa. Over the period 1996-2014 we identify 3174 days, an average of 167 days per year, when the air-mass over the
Caribbean sites could be linked to at least one of the two West African sites. For 1162 of these days, AOD data are available
for the Caribbean sites as well as for the corresponding West African sites about 5-7 days earlier, when the air mass
overpassed these sites. We identified dust outbreaks as those air masses yielding $AOD \geq 0.2$ and an Ångström Exponent
below 0.6. On this basis of the total 1162 days, 484 meet the criteria for mineral dust outbreaks. Comparing the AOD
25 properties over Africa and those over the Caribbean we observe the following changes in aerosol-related properties: AOD at
440nm decreases about 0.16 or -30%. The volume particle size distribution shows a similar decrease in the volume
concentration, mainly in the coarse mode. The single scattering albedo, refractive indexes, and asymmetry factor remain
unchanged. The difference in the effective radius over West African sites with respect to Caribbean sites ranges between 0
and -0.3 μm . Finally we conclude that in about half of the cases only non-spherical dust particles are present in the
30 atmosphere over the African and Caribbean sites, while in the other cases dust particles were mixed with other types of
aerosol particles.

1 Introduction

Mineral dust is one of the most abundant aerosol types in the global atmosphere and as such it could play an important role in climate. Mineral dust absorbs and scatters terrestrial and solar radiation and thus affects the Earth's radiation budget (Chooari et al., 2014). Dust is also involved in cloud microphysical processes which in turn affect radiation properties and the hydrological cycle (Karydis et al., 2017; DeMott et al., 2010). Dust also serves as a major source of nutrients to ocean and terrestrial ecosystems and in this way dust deposition can impact the carbon cycle (Jiskels et al., 2005). All these processes could have a significant impact on climate. Given the importance of dust there is a need to understand the factors affecting African dust source activity and the properties of the dust so produced and how those properties change during transport. Africa is the world's largest dust sources, estimated to produce over half the global total (Huneeus et al., 2011). Much African dust is transported to the west and significant quantities reach South America (Prospero et al., 2014; Yu et al., 2014, 2015), the Caribbean Sea (Prospero and Lamb, 2003), and southern United States (Bozlaker et al., 2013).

Studies of the dust transport from Africa to the Americas have been carried out using meteorological information linked to *in-situ* and satellite aerosol data (e.g., Jickells et al., 2005; Rodríguez et al., 2015; García et al., 2017). Recently developed techniques such as MACC (Monitoring Atmospheric Composition and Climate; Chouza et al., 2016) or MOCAGE (Modélisation de la Chimie Atmosphérique Grande Echelle; Martet et al., 2009) models have been also used to monitor dust plumes.

Long-term (e.g., Prospero and Lamb, 2003; Prospero and Mayol-Bracero, 2013) and short-term (e.g., Reid et al., 2003; Colarco et al., 2003; Kaufman et al., 2005; Valle-Díaz et al., 2016) studies show a seasonal dependence in the intensity of dust transport to the Caribbean with the greatest transport in boreal summer. In the SALTRACE program (Weinzierl et al., 2017) an aircraft was used to carry out atmospheric column closure experiments performed in June and July 2013 at West African and Caribbean sites. A unique Lagrangian *in-situ* study was carried out in SALTRACE wherein a dusty air mass was sampled aboard an aircraft over the Cape Verde Islands and again five days later over Barbados, a distance of more than 4,000 km. They measured a distinct change in particle size during transit across the Atlantic and noted that the removal rate of large super-micron particles was slower than expected based on simple sedimentation calculations (Weinzierl et al., 2017). Similar results had been obtained on comparisons between surface based measurements at sites in the Canary Islands and Puerto Rico. (Maring et al., 2003).

Our study is inspired in that experiment, although our approach is to use columnar aerosol data collected from CIMEL sun-photometers of the AERosol RObotic NETwork (AERONET) in the two areas, West Africa and on islands in the eastern Caribbean. The temporal coverage of the AERONET data is large – at one site, 19 years from 1996 to 2014. Therefore, the

aim of this work is to investigate the changes in dust optical and microphysical properties due to the long-range transport, by comparing AERONET observations in West Africa and the Caribbean sites using a climatological approach.

In Section 2 we present an overview of the database and methodology used to match daily-averaged AERONET data at both sides of the Atlantic Ocean using air mass backwards trajectories. Section 3 describes, separately, the long-term aerosol climatology observed at the West Africa and the Caribbean sites and the correlation between AOD and Dust concentration observed at the Caribbean sites. Section 4 presents the monthly variability of aerosol size parameters. Section 5 presents the air mass Caribbean-African connection climatology, as well as the change in aerosol optical depth, size distribution, and single scattering albedo, among others after the long-range transport. Finally the conclusions are presented in Section 6.

2 Database and Methodology

10 2.1 AERONET measurements and sites

The main database for this study includes the daily mean values of columnar aerosol data measured by CIMEL CE-318 Sun photometer in the AERONET framework (Holben et al., 1998). The direct sun algorithm provides a database that contains instantaneous values (every 15 minutes) of spectral AOD at 7 wavelengths in the range 340nm – 1020nm (in some cases also 1640nm depending on the instrument model) and the associated Ångström Exponent (AE) based on the wavelengths 440 and 870 nm. We only use AOD and AE quality assured cloud-screened level 2.0 data (version 2) which ensures the reliability of the measurements. In this work we use only the 440 nm measurements. Figure 1 and Table 1 present the five AERONET sites in the Caribbean (CAR) zone and the two sites in the West African (AF) zone chosen in this study.

In addition the CIMEL instrument makes hourly measures of sky radiances in almucantar geometry at certain wavelengths in the range 440-1020 nm (in some cases also 1640nm, number of wavelengths depending on the instrument model). The sky radiances, together with the AOD, are used to derive optical and microphysical properties of the aerosol using inversion procedures (Dubovik et al., 2006). The inversion-derived parameters used in this study are: Volume Particle Size Distribution (VPSD) and the volume concentration for the fine, coarse and total size distribution (VC_F , VC_C , VC_T , respectively), Sphericity fraction (SF), Total Effective Radius (ER_T), Real Refractive Index (REFR), Imaginary Refractive Index (REFI), Single Scattering Albedo (SSA), and Asymmetry Parameter (g).

The Level 2 inversion requirement rejects AOD values less than 0.4 which dramatically reduces the amount of data. In order to increase the number of measurements in the data set we used level 1.5 inversion products but we applied an extra level of quality control to ensure the reliability of the inversion data:

- VPSD and ER_T : same as AERONET level 2.0 criteria (solar zenith angle $>50^\circ$, number of symmetrical angles, and sky error between 5% and 8% depending on AOD, see http://aeronet.gsfc.nasa.gov/new_web/Documents/AERONETcriteria_final1_excerpt.pdf), but without threshold with respect to AOD.

- SSA, g, REFR, REFI and SF: same as AERONET level 2.0 criteria but with $AOD \geq 0.20$ (see Dubovik et al., 2006; Mallet et al., 2013; Mateos et al., 2014) instead of >0.4 .

The use of level 1.5-filtered data with an extra quality control has been previously used by other authors (e.g., Burgos et al., 2016) with no loss of accuracy (Mateos et al., 2014). All the available inversion products are daily averaged in this study.

- 5 With the threshold of $AOD \geq 0.2$, estimated uncertainty for dust retrievals of the single scattering albedo is 0.03, real refractive index is 0.04, imaginary refractive index is 50%, and the volume particle size distribution is 35% (see Dubovik et al., 2000). The climatology of key aerosol properties measured at West African and Caribbean sites is addressed in Section 3. All daily available records (see Table 1) in the two West African and five Caribbean sites are averaged in the 1996-2014 period, resulting two databases with 5656 and 5099 days of data, respectively.

10 **2.2 Linkage between Caribbean and West Africa by air mass back-trajectories**

All the air mass links between West African and Caribbean sites are searched. This task requires the separate analysis for each Caribbean site. For example, the methodology used in this study for Barbados is the following:

- **Step1:** We calculated three-dimensional 10-day back-trajectories with 1-hour time resolution using the Hybrid Single Particle Lagrangian Integrated Trajectory Model (HYSPLIT) version 4.0 (Stein et al., 2015). The geographical coordinates used as the start point are presented in Table 1. As mineral dust can be transported at altitude levels higher than the boundary layer, most notably in the Saharan Air Layer (Carlson and Prospero, 1972; Yu et al., 2014; Groß et al., 2016), back-trajectories were calculated at 750, 2500 and 4500 m (a.g.l.). The core of the SAL is typically at around 2500m. For the trajectory vertical motion, we used the model vertical velocity. The meteorological database used as input for HYSPLIT is the NCAR/NCEP global Reanalysis (Kalnay et al., 1996).
15 The evaluation is performed for each day in the period 1996-2014 at 16:00 UTC (around local noon).
- **Step2:** If any of these trajectories (at one, two or three heights) passes through a $3^\circ \times 3^\circ$ box centered on the West African sites - we consider that a link has been established between the two sites. The transit time is typically about 5 – 7 days. In some cases an air mass back-trajectory may link both the Capo_Verde and Dakar boxes. In such cases the mean of the aerosol observations is used.
- **Step3:** Once the dates in which the air mass is measured in Barbados and in Capo_Verde or Dakar (or both) sites are established, the associated AERONET aerosol data are identified. In the case of Barbados site, the corresponding daily means of all AERONET products are used. However, the West African site analysis requires a special procedure. The visual inspection of many of the cases shows that the aerosol records for the specific date obtained in the trajectory analysis often fell on a day without data (e.g., due to cloudy or rainy conditions) or did not capture the central days of the dust event. To resolve this problem, we introduced a ± 1 day adjustment to the back-trajectory estimated date at Capo_Verde and Dakar. This is in line with previous studies which state that desert dust episodes in West African sites usually last for several days (e.g., Knippertz and Stuu, 2014). The aerosol values for each West African site are therefore averaged over the three days (the estimated date and ± 1 day). For the Barbados-African
25
30

cases with air masses overflowing both Capo_Verde and Dakar sites, the corresponding average of aerosol data is used.

These three steps described above are applied to all Caribbean sites as shown in Table 1. This methodology yields five databases (one per site) in which each Caribbean site is linked with an data for African sites. For each day between 1996 and 2014 we determine which Caribbean sites present an air mass link with West African sites. If more than one African site yields a link n for a specific Caribbean event, we use the mean properties as discussed above.

We identify a desert dust event on the basis of the following criteria: $AOD \geq 0.2$ and $AE \leq 0.6$ (e.g., Dubovik et al., 2002; Guirado et al., 2014). In the evaluated global Caribbean-African linked database, the Caribbean and African data are analyzed separately. Hence, there are two different inventories that contain all days meeting the criteria for mineral dust events over the Caribbean and West African sites. In the global database there are, therefore, three different cases which are extensively analyzed in Section 5:

- a) $D_{AF} + D_{CAR}$: Desert dust conditions occur in both Caribbean and West African sites
- b) $D_{AF} + NoD_{CAR}$: Dust condition in West African sites but no-dust condition in the Caribbean sites
- c) NoD: No-dust conditions

We found a total of 3174 days showing connection between West African and Caribbean sites. Only 1162 out of 3174 days yielded AERONET data (level 2.0) for AOD and AE. Of these 1162 acceptable days, 484 meet the criteria for mineral dust outbreaks ($AOD \geq 0.2$ and $AE \leq 0.6$, " $D_{AF} + D_{CAR}$ " case). However for the analysis of microphysical and radiative properties, the number of matching inversion data is however much smaller (just 71 cases) because of the more stringent requirements. The frequent cloudiness at the Caribbean sites is the main difficulty in the inversion of sky radiances (see Table 1).

3 Seasonal variability of aerosol load at the West African and Caribbean sites

In this section the analysis of the monthly-seasonal cycle of the main aerosol properties in the Caribbean and African sites is presented separately since there is no requirement that trajectories connect the sites. This section summarizes overall multi-year statistics (from 1996 to 2014) of AOD, AE and VPSD quantities.

Figures 2 and 3 present the multiannual AOD and AE monthly averages of 19 years in West African and Caribbean regions, respectively. There is a significant difference between the "cold" (October-April) and "warm" (May-September) seasons in both areas. We have held here the usual cold-warm season distinction in northern hemisphere areas, but there is not that difference in temperature seasonal cycle in the Caribbean Basin.

In the winter season there is a weak variation of AOD and AE at the West African sites (see Figure 2) with values around 0.3 and 0.3-0.5, respectively. In contrast in the summer season there is an increase of AOD together with a decrease of AE until

June when the maximum of AOD (0.6) coincides with a minimum of AE (0.16). The AOD peak was also observed by, e.g., Tegen et al. (2013). After June there is a progressive decrease of AOD values and increase in AE until once again reaching winter levels. Overall, the large AOD and low AE values suggest dominant effect of coarse particles in dust episodes. The ranges of AOD between 0.3 and 0.6 and AE below 0.5 were also obtained by previous studies in West African sites (e.g.,
5 Dubovik et al., 2002; Horowitz et al., 2017). Haywood et al., (2008), Derimian et al., (2008), and Leon et al. (2009) reported that M'Bour site (western Senegal, 70km away from Dakar) is under the major influence of desert dust throughout the year. The effects of biomass burning are seen in November and December when AE reaches its maximum of about 0.5; this is the time of year when biomass burning is at a maximum in the Sahel.

10 The annual cycle of AOD in the Caribbean sites (see Figure 3) shows a bell shape with the maximum in June (AOD = 0.3) and the minimum values in December-January. In contrast, the AE displays a larger variability along the year: an increase from January to April when AE = 0.7 (the annual maximum), followed by a steady sharp decline until the absolute minimum in June-July with AE= 0.26. Levels remain constant around 0.55 from September to December. These features in the AOD
15 and AE seasonality can be understood as the fingerprint of the occurrence of mineral dust transport from Africa. The AE variability evidenced by the standard deviations is large driven by the changes in aerosol mixture that occur in this area (e.g., Reid et al., 2003). Clean maritime conditions, associated to background values, have low AOD and low AE (Smirnov et al., 2000), but they can be modified by mineral dust outbreaks from African deserts and biomass burning episodes. In particular, the large change in AE in the "cold" season is largely due to the advection of pollutant aerosols from higher latitudes (e.g., Savoie et al., 2002; Zamora et al. 2013).

20 Previous work (e.g., Smirnov et al., 2000) has shown that high concentrations of dust at the surface are correlated with high column optical depths measured by a collocated AERONET instrument. Yu et al. (2014) has shown that CALIPSO (Cloud-Aerosol Lidar and Infrared Pathfinder Satellite Observations) dust concentrations over Barbados track the surface-based measurements of dust. As a first step we show the relationship between the long-term measurements of dust concentrations at the surface with the columnar aerosol load manifested in AOD. We use the surface dust concentration measured at Ragged
25 Point, Barbados, site (e.g., Prospero and Lamb, 2003; Prospero and Mayol, 2013) between 1996 and 2011. Daily surface dust concentrations are obtained with high volume filter samplers using measured aluminum concentrations and assuming an Al content of 8% in soil dust (e.g., Prospero, 1999) or from the weights of filter samples ashed at 500° C after extracting soluble components with water (Prospero, 1999; Prospero et al., 2014; Savoie et al, 2002)).

Surface dust concentration seasonal cycle (Figure 3) presents a significant increase between low values during October-April season up to larger concentrations in May-September season. Overall, the shapes of the annual cycles of AOD and surface
30 dust concentration at Barbados are similar and the same seasonal pattern in both variables is observed.

Monthly mean AOD is highly correlated with surface dust concentrations as shown in Figure 4 which is based on 3700 pairs of daily data, a total of 192 monthly mean, and 12 inter-annual monthly mean values, the latter calculated as the average of

the available daily data from the same month over a multi annual period. The seasonal distribution of the surface-columnar values seems to follow a linear increasing pattern from winter (bluish colors) to summer (reddish colors). The slope of the fit between dust concentration and AOD is about $115 \mu\text{g m}^{-3}$ per unit of AOD for the two cases analyzed here: using 192 monthly means (Figure 4a) and 12 inter-annual monthly means (Figure 4b). The Barbados dust concentration vs AOD shows very good correlation when the same months are averaged along the years. However, the monthly agreement between these two variables displays a certain degree of dispersion with a moderate correlation coefficient. The positive intercepts on AOD in the fits are most likely attributable to the effects of sea salt aerosol on AOD.

4 Monthly variability of size-related aerosol parameters

Figure 5 displays the average monthly cycle of the volume particle size distribution (VPSD) for the West African and Caribbean sites, respectively. These figures are based on 3346 and 2165 daily mean values of the AERONET inversion products selected as described above.

The coarse mode predominance can be observed throughout the year in both areas. The seasonal cycle of VPSD in West African sites (Figure 5a) shows a clear change of coarse mode concentration throughout the year, although the coarse mode effective radius does not change, with peak concentration of the coarse mode about $2.24 \mu\text{m}$. The coarse mode concentration ranges between maximum values in June with $0.32 \mu\text{m}^3/\mu\text{m}^2$ and minima in November-December with $0.05 \mu\text{m}^3/\mu\text{m}^2$. In terms of volume concentration the fine mode plays an almost negligible role throughout the year for the “ $D_{\text{AF}} + D_{\text{CAR}}$ ” cases. This seasonal pattern was already reported by previous studies in the West African sites (e.g., Dubovik et al., 2002; Eck et al., 2010; Guirado et al., 2014). These studies showed the domination of large particles (i.e., radius greater than $0.6 \mu\text{m}$) with VPSD peaks in the coarse mode at $2 \mu\text{m}$, which are independent of the aerosol load.

The conditions observed at the Caribbean sites (Figure 5b) show a change in the mean size of the aerosol particles during the course of the year. In the "warm" season (May-Sep) the maximum concentration peaks about $2.24 \mu\text{m}$ radius identical to the coarse mode size distribution found at the West African sites (Fig. 5a), although the concentration values are lower (as is AOD). In the "cold" season (Oct-Apr), however, the coarse mode maximum concentration is achieved at larger radius (about $3.85 \mu\text{m}$) highlighting the predominance of large sea salt particles. This difference in the coarse mode radii between marine aerosol and dust has been observed in other coastal locations affected by dust outbreaks (e.g., Prats et al., 2011). In addition, the maximum volume concentration of the coarse mode exhibits maximum values in June with $0.12 \mu\text{m}^3/\mu\text{m}^2$ and minimum ones in November-December with $0.02 \mu\text{m}^3/\mu\text{m}^2$. In terms of volume concentration the fine mode plays a minor role throughout the year in the Caribbean sites. The entire size range of VPSD in the "cold" season is in line with previous studies carried out in oceanic environments (e.g., Dubovik et al., 2002) with low particle volume concentrations peaking at very large radius ($> 3 \mu\text{m}$).

5 Air Mass Connections between African and Caribbean areas

In this section, we select only those days when the back trajectories link African sites with Caribbean sites as explained in Section 2.2. In this way, the aerosol properties observed in the Caribbean sites can be compared those observed 5 – 7 days earlier over the West African sites.

5.1 Air-mass African and Caribbean connections: all data and dusty data

Following the methodology described in the Steps 1 and 2 of Section 2.2, we obtained a list of days when Caribbean air masses could be linked to West Africa. Figure 6 shows the seasonal cycle of the total number of days with this connection in the period 1996-2014. Overall, almost half of the days each year (~167 days per year) display a Caribbean-African linkage with a total of 3174 cases in 19 years.

10

The total number of air mass connections between both areas exhibits small values from January through April with an absolute minimum in April with only 2 days per month. This minimum at the Caribbean sites coincides with the minimum in aerosol load observed in the seasonal cycle at the West African sites (see Figure 2).

With the beginning of the "warm" season (May-September) the number of connections shows a notable increase achieving its maximum in July with almost all the days at the Caribbean sites being connected with those in West African. From October to December there is a progressive decline in links from 20 to 10 days per month.

Unfortunately, columnar aerosol data are not available for each of the 3174 connection days. A total of 1162 out of 3174 days (36% of the total) are present in AERONET data of level 2.0 (see Section 2.2). Furthermore, only 484 cases (15% of the total) meet the dusty criteria in both areas (case " $D_{AF} + D_{CAR}$ ") described in Section 2.2). This is due to the limitation in the data coverage and to the strict criteria used to unambiguously identify desert dust events. It should be noted that this procedure underestimates the actual number of desert dust events observed by ground-based measurements. For instance, during June-July-August in the Caribbean sites there is essentially continuous dust (e.g., Prospero et al., 2015), which is corroborated in this study with an average of 23-28 connection days in these months.

20

5.2 Scatterplot AE-AOD in the African and Caribbean areas

The next step focuses on the comparison of the aerosol properties observed in the Caribbean sites and the values of the same properties which were observed 5 – 7 days before over the West African sites. In this way, the impact of the long range transport can be quantified. Figure 7 presents the scatterplot AE-AOD for those days with aerosol data and air mass links between the two areas. When the criteria for identifying mineral dust ($AOD \geq 0.2$ and $AE \leq 0.6$) are applied to the global Caribbean-African connected database, three different cases are identified (see Section 2.2).

In the West African sites (Fig. 7a), as expected because of the proximity to the Saharan Desert, the influence of the mineral dust aerosol properties is predominant: 86% of the available data have $AOD \geq 0.2$ and $AE \leq 0.6$, (1000 out of 1162 days).

30

We identified the occurrence of 498 dusty days in the Caribbean sites, about 42% of the entire global Caribbean-African connected database, but just 484 days (in the period 1996-2014) are shown to be dusty days in the Caribbean sites with aerosol origin in the Saharan desert (indicated as a “ $D_{AF} + D_{CAR}$ ” case in Figure 7). Intense dusty days (AOD larger than 0.5) occur in West African and Caribbean sites in 430 and 67 cases, respectively. This difference is attributable to a decrease in aerosol load during transport between the two regions. Out of the total of 1162 cases 516 meet the dusty criteria only in the African database (“ $D_{AF} + NoD_{CAR}$ ” case in figure 7). This decrease in dust loads is also observed in the change of the AE and AOD using ground-based and satellite measurements (see, e.g., Yu et al., 2014). For instance, there are 102 cases in the Caribbean database where $AE > 0.6$ whereas the same air mass yielded $AE < 0.6$ in the West African sites days before. In addition, there are possible misidentifications of dusty days with AOD and AE values close to the required thresholds (156 and 59 days in the interval of $0.15 < AOD < 0.20$ in the Caribbean and West African sites, respectively). This misidentification can also occur in the “NoD” case, when no dust is observed. We considered lowering the AOD threshold so as to lower values so as to include more cases but this would reduce confidence about the actual presence of dust.

5.3 Differences between AOD in the West African and the Caribbean sites

Once the connections have been detected, changes in AOD due to the long-range transport over the Atlantic Ocean are studied depending on the AE values. The results are shown in Figure 8. The AOD_{CAR} has been plotted as a function of AOD in the West African sites (AOD_{AF}).

The scatter plot in Fig. 8 shows that there is, as expected, a decrease in AOD in air masses transiting the Atlantic. The mean decrease of AOD between West African and Caribbean sites is 0.16, a decrease of about 30% with respect to the values at Dakar and Cabo Verde. They are greatest for cases where AOD values are large ($AOD > 0.8$) at the West African sites, with decreases up to 70%. In the interval $0.5 < AOD < 0.8$ the decreases are in the range about 28-45% while those in the interval $0.2 < AOD < 0.5$ are in the range 11-27%. These percentages based on long-term and ground-based data are a first approach to assess the estimations done by studies dealing with satellite data. For instance, Yu et al. (2015) have reported, in a latitudinal belt of $10^{\circ}S-30^{\circ}N$, a loss of 70% ($\pm 45-70\%$) between dust amount (in $Tg\ y^{-1}$) leaving West Africa (at $15^{\circ}W$) and the end of the Caribbean sites (at $75^{\circ}W$). Hence, our estimations are in line with these findings considering that the measured variable and studied area are not identical.

The cases with low AE values are those cases with a wider variability in AOD difference. In addition, there are some cases in which AOD is larger in the Caribbean sites. This effect could be explained by different reasons: inhomogeneity of the dust layer, addition of other aerosol particles in the Caribbean sites, temporal gaps in the instantaneous measurements that cause non-representative daily averages, and cloud contamination not detected by the cloud-screening algorithm, etc.

5.4 Aerosol microphysical properties for African-Caribbean Sea connections

In this section we focus on the key aerosol microphysical properties for those cases where we found a link between the West African and Caribbean sites. Figure 9 shows the VPSD for the case analyzed before: dust conditions in both areas (“ $D_{AF} + D_{CAR}$ ”). The main characteristics of the VPSD curve for this collection of data in the African side are the same as described in detail in Section 4. The fine mode volume fraction (obtained as the ratio VC_F/VC_T) is on average as low as 0.077. The VPSD in the Caribbean sites for the “ $D_{AF} + D_{CAR}$ ” case is similar to that in the West African sites: average coarse mode volume concentration of $0.22 \mu\text{m}^3/\mu\text{m}^2$, maximum peak about $2.24 \mu\text{m}$ radius, and very low fine mode concentration (average of $0.02 \mu\text{m}^3/\mu\text{m}^2$ peaking at $0.086 \mu\text{m}$, fine mode volume fraction of 0.09). The coarse mode volume concentration decreases from $0.34 \mu\text{m}^3/\mu\text{m}^2$ in West Africa to $0.22 \mu\text{m}^3/\mu\text{m}^2$ in the Caribbean sites. Hence, there is a loss about 35% in the coarse mode concentration between both areas caused by the long-range transport over the Atlantic Ocean.

To quantify the change in the mean aerosol size caused by the long-range transport, Figure 10 shows the histogram of the differences between the effective radius of the total size distribution (ER_T) in the two areas. On average, ER_T shows values of 0.88 and $0.76 \mu\text{m}$ in West African and Caribbean sites, respectively. Most of the differences in the ER_T values are negative, thus indicating the size distribution in West Africa generally having larger particles than in the Caribbean sites. The differences in the effective radii are mostly confined (about 70% of the cases) between no change and a decrease in the effective radius about $0.3 \mu\text{m}$ between both areas. The maximum of occurrence is found for a decrease about $0.2 \mu\text{m}$. Positive differences (15% of the cases), meaning larger particle size in the Caribbean sites, could be attributed to the presence of other aerosol layers (e.g., sea salt) in the atmospheric column. Uncertainties of the inversion could also explain the positive differences.

The third microphysical property studied in this study is the fraction of spherical particles found in the inversion process. In the retrieval, particles are modeled both as spheres and spheroids, and the inversion finds which fraction of spherical and non-spherical particles (defined by aspect ratios) better fits to the observations (for details, see Dubovik et al., 2006). The results are presented in Figure 11. This figure shows that in the West African sites there is large predominance of non-spherical particles, that is $SF < 0.05$. Respectively about 80% and 53% of the values in the West African and Caribbean sites were completely non-spherical. Overall, in 32 out of 71 cases (45%) there is no change between both areas and the shape of the particles is predominantly non-spherical. Cases with sphericity fraction below 0.05 in West African sites display a wide variability in the observed fraction in the Caribbean sites, even achieving values of 0.7. This increase could be explained by the mixture of mineral dust with other (spherical) aerosol particles, such as maritime aerosols. Note that we use column observations; therefore the mixture in this case does not mean that dust and other aerosol particles are necessarily in the same layer; they can be separated in different atmospheric layers. For instance, during SALTRACE experiment the main four dust events recorded presented a vertical structure with up to three layers: the boundary layer, the entrainment or mixing layer and the pure Saharan dust layer (Groß et al., 2015). Uncertainties of the inversion method can also be a reason for the high

fraction of spherical particles. The *in situ* measurements at Barbados collect dust in the boundary layer (Prospero, 1999; Smirnov et al., 2000; Yu et al., 2014), so that dust is collected simultaneously with sea-salt and other aerosol types (e.g., Ansmann et al., 2009; Toledano et al., 2011; Groß et al., 2011). There is a correlation between high *in situ* dust mass concentrations, high total aerosol optical depth, and low Angström exponent (Groß et al., 2016). However the highest concentrations of dust are found in the elevated Saharan Air Layer (Yu et al., 2014) where there are no significant concentrations of sea salt aerosol (Savoie et al., 2002).

5.5 Aerosol radiative properties for African-Caribbean Sea connections

Figure 12 compares the main radiative properties (SSA, g , REFR, and REFI) at the Caribbean and African sites to assess changes in optical properties that occur after long-range transport. SSA in Figure 12a and REFI in Figure 12c are the same in both areas within the limits of uncertainty. The SSA at Dakar and Cabo Verde increases with wavelength: from 0.94 at 440 nm up to 0.98 at 670, 870, and 1020 nm. These figures are in line with previous studies in this area (Dubovik et al., 2002; Eck et al., 2010; Kim et al., 2011; Toledano et al., 2011; Giles et al., 2012, among others) and also with measurements at various Spanish and Mediterranean sites during desert dust outbreaks (e.g., Meloni et al., 2006; Cachorro et al., 2010; Valenzuela et al., 2012; Burgos et al., 2016). The SSA in dust events in the Caribbean sites is essentially identical to that at the West African sites. The same is true for REFI: 0.0025 at 440 nm and 0.001-0.0015 in the interval 670-1020 nm. The values in the visible and near infrared ranges are slightly larger than those reported by Dubovik et al. (2002) which were about 0.0007; their value at 440 nm is very similar to the value we present here. There is no significant change in the REFR either, being the mean real part of the refractive index in the African and Caribbean database, about 1.45 ± 0.01 . This value is slightly lower than the reported by Dubovik et al. (2002) which was about 1.48. Finally, the asymmetry factor g at 440 nm decreases slightly from 0.77 in West African sites to 0.755 in the Caribbean sites. The g values reported in this study are slightly larger than the reported by previous studies for desert dust in Africa (e.g., Dubovik et al., 2002). Overall, the intensive optical properties (both absorption and scattering quantities) do not change significantly in spite of the long range transport.

6 Conclusions

The objective of this study was to characterize changes in aerosol physical-radiative properties that occur in dust-laden air masses that transit the Atlantic from Africa to the eastern Caribbean. To this end we compared AERONET sun photometer measurements and inversion products made over the period 1996-2014 at five island sites in the eastern Caribbean with those made at two sites in the eastern Atlantic. Focusing first on the results from the two African sites, we find that the dust properties are quite similar from event to event. This suggests that while specific dust events may indeed have characteristic signature properties at the time the dust is generated over the interior of North Africa, by the time the dusty air mass reaches the coast that signature has been lost and those properties have become homogenized.

We focused efforts on paired measurements made on the same dust outbreaks in a procedure that identified trajectories from the Caribbean island sites that back-tracked to one or both of the African sites. We find that there is no substantial change in the intensive radiative properties in African air masses after a journey of 5 – 7 days over a distance of 4000km. There is a decrease of about 30% in the coarse mode concentration of the size distributions but the coarse mode effective radius does not change. Non-spherical particles characteristic of dust are the predominant shape in both areas. In general there were no substantial changes in the spectral dependence of the absorbing and scattering properties of dust during transit.

Our findings that suggest uniformity in properties are similar to those reached in Bozlaker et al., 2017 who measured the concentrations and isotopic composition of a broad suite of elements in Barbados dust samples collected in 2013 and 2016. Although dust concentrations were highly variable, the elemental and isotopic abundances fell in a relatively narrow range compared to wide-ranging compositions reported for hypothesized dust sources in North Africa. In contrast the Barbados composition was very similar to that reported in the literature for samples collected at sites on the coast of West Africa on islands or ships close to the coast. These results suggest that during large dust events, the dust from different sources which may have different signatures becomes homogenized during transport from the interior of North Africa to the coast and that there is relatively little change in dust properties during transit of the Atlantic.

The results of our study and that of Bozlaker et al. suggest that the modeling of the radiative effects of dust over the Atlantic can be simplified in that it can be assumed that the radiative properties of dust are relatively uniform and unchanging during transport within the context of the range of properties discussed here.

20 **Acknowledgments**

The authors gratefully acknowledge the NASA AERONET program for the very valuable data used in this study. We thank Brent Holben (Barbados, La_Parguera), Didier Tanre (Capo_Verde, Dakar), and Olga Mayol-Bracero (Cape San Juan) for their effort in establishing and maintaining their sites. This work has received funding from the European Union's Horizon 2020 research and innovation programme under grant agreement N° 654109 (ACTRIS-2). The authors are grateful to Spanish MINECO for the financial support of the IJCI-2014-19477 grant, PTA2014-09522-I grant, and POLARMOON project (ref. CTM2015-66742-R). We also thank 'Consejería de Educación' of 'Junta de Castilla y León' for supporting the GOA-AIRE project (ref. VA100P17). Prospero received support from NSF AGS-0962256 and NASA NNX12AP45G.

References

- Ansmann, A., Baars, H., Tesche, M., Müller, D., Althausen, D., Engelmann, R., Pauliquevis, T., and Artaxo, P.: Dust and smoke transport from Africa to South America: Lidar profiling over Cape Verde and the Amazon rainforest, *Geophys. Res. Lett.*, 36, L11802, doi:10.1029/2009GL037923, 2009.
- 5 Bozlaker, A., Prospero, J. M., Fraser, M. P., and Chellam, S.: "Quantifying the contribution of long-range Saharan dust transport on particulate matter concentrations in Houston, Texas, using detailed elemental analysis." *Environmental Science and Technology* 47 (18):10179-10187. doi: 10.1021/es4015663, 2013.
- Bozlaker, A., J. M. Prospero, J. Price, and S. Chellam (2017), Linking Barbados Mineral Dust Aerosols to North African Sources Using Elemental Composition and Radiogenic Sr, Nd, and Pb Isotope Signatures, *Journal of Geophysical Research: Atmospheres*, 123, 1384-1400, doi:10.1002/2017JD027505.
- 10 Burgos, M.A., Mateos, D., Cachorro, C., Toledano, C., and de Frutos, A.M.: Aerosol properties of mineral dust and its mixtures in a regional background of north-central Iberian Peninsula, *Science of the Total Environment* 572, 1005-1019, 2016.
- Cachorro, V. E., Toledano, C., Antón, M., Berjón, A., de Frutos, A.M., Vilaplana, J. M., Arola, A., and Krotkov, N.A.: Comparison of UV irradiances from Aura/Ozone Monitoring Instrument (OMI) with Brewer measurements at El Arenosillo (Spain) – Part 2: Analysis of site aerosol influence. *Atmos. Chem. Phys.* 10, 11867-11880. doi:10.5194/acp-10-11867-2010, 2010.
- 15 Cachorro, V. E., Burgos, M.A., Mateos, D., Toledano, C., Bennouna, Y., Torres, B., de Frutos, A.M., and Herguedas, A.: Inventory of African desert dust events in the North-central Iberian Peninsula in 2003-2014 based on Sun photometer and PM_x data. *Atmos. Chem. Phys.* 16, 8227-8248. doi:10.5194/acp-16-8227-2016, 2016.
- Carlson, T. N., and Prospero, J. M.: The Large-Scale Movement of Saharan Air Outbreaks over the Northern Equatorial Atlantic. *J. Appl Meteorol.* 11 (2):283-297, 1972.
- Choobari, O. A., P. Zawar-Reza, A. Sturman (2014): The global distribution of mineral dust and its impacts on the climate system: A review. *Atmos. Res.* 138(0), 152-165. doi: 10.1016/j.atmosres.2013.11.007.
- 25 Chouza, F., Reitebuch, O., Benedetti, A., and Weinzierl, B.: Saharan dust long-range transport across the Atlantic studied by an airborne Doppler wind lidar and the MACC model, *Atmos. Chem. Phys.*, 16, 11581-11600, doi:10.5194/acp-16-11581-2016, 2016.
- Colarco, P., Toon O., and Holben B.: Saharan dust transport to the Caribbean during PRIDE: 1. Influence of dust sources and removal mechanisms on the timing and magnitude of downwind aerosol optical depth events from simulations of in situ and remote sensing observations, *J. Geophys. Res.*, 108(D19), 8589, doi:10.1029/2002JD002658, 2003.
- 30 DeMott, P. J., A. J. Prenni, X. Liu, S. M. Kreidenweis, M. D. Petters, C. H. Twohy, M. S. Richardson, T. Eidhammer, and D. C. Rogers (2010), Predicting global atmospheric ice nuclei distributions and their impacts on climate, *Proceedings of the National Academy of Sciences*, 107(25), 11217-11222, doi:10.1073/pnas.0910818107.

- Derimian, Y., Leon, J.-F., Dubovik, O., Chiapello, I., Tanré, D., Sinyuk, A., Auriol, F., Podvin, T., Brogniez, G., and Holben, B.: Radiative properties of aerosol mixture observed during the dry season 2006 over M'Bour, Senegal (African Monsoon Multidisciplinary Analysis campaign), *J. Geophys. Res.*, 113, D00C09, doi:10.1029/2008JD009904, 2008.
- Dubovik, O., Smirnov, A., Holben, B., King, M.D., Eck, T.F., Kaufman, Y.J., and Slutsker, I., and Eck, T. F.: Accuracy assessments of aerosol optical properties retrieved from Aerosol Robotic Network (AERONET) Sun and sky radiance measurements. *J. Geophys. Res.*, 105(D8), 9791-9806, 2000.
- Dubovik, O., Holben, B., Eck, T.F., Smirnov, A., Kaufman, Y.J., King, M.D., Tanre, D., and Slutsker, I.: Variability of absorption and optical properties of key aerosol types observed in worldwide locations. *J. Atmos. Sci.* 59, 590–608, 2002.
- Dubovik, O., Sinyuk, A., Lapyonok, T., Holben, B.N., Mishchenko, M., Yang, P., Eck, T.F., Volten, H., Munoz, O., Veihelmann, B., van der Zande, W.J., Leon, J.F., Sorokin, M., and Slutsker, I.: Application of spheroid models to account for aerosol particle nonsphericity in remote sensing of desert dust. *J. Geophys. Res.-Atmos.* 111 (D11), 2156-2202. doi:10.1029/2005JD006619, 2006.
- Eck, T. F., Holben, B. N., Sinyuk, A., Pinker, R. T., Goloub, P., Chen, H., Chatenet, B., Li, Z., Singh, R. P., Tripathi, S. N., Reid, J. S., Giles, D. M., Dubovik, O., O'Neill, N. T., Smirnov, A., Wang, P., and Xia, X.: Climatological aspects of the optical properties of fine/coarse mode aerosol mixtures. *J. Geophys. Res.* 115, D19205. doi:10.1029/2010JD014002, 2010.
- García, M. I., Rodríguez, S., and Alastuey, A.: Impact of North America on the aerosol composition in the North Atlantic free troposphere, *Atmos. Chem. Phys.*, 17, 7387-7404, <https://doi.org/10.5194/acp-17-7387-2017>, 2017.
- Giles, D. M., Holben, B. N., Eck, T. F., Sinyuk, A., Smirnov, A., Slutsker, I., Dickerson, R. R., Thompson, A. M., and Schafer, J. S.: An analysis of AERONET aerosol absorption properties and classifications representative of aerosol source regions. *J. Geophys. Res.* 117, D17203. doi:10.1029/2012JD018127, 2012.
- Groß, S., Freudenthaler, V., Schepanski, K., Toledano, C., Schäfler, A., Ansmann, A., and Weinzierl, B.: Optical properties of long-range transported Saharan dust over Barbados as measured by dual-wavelength depolarization Raman lidar measurements, *Atmos. Chem. Phys.*, 15, 11067-11080, doi:10.5194/acp-15-11067-2015, 2015.
- Groß, S., Tesche, M., Freudenthaler, V., Toledano, C., Wiegner, M., Ansmann, A., Althausen, D. and Seefeldner, M.: Characterization of Saharan dust, marine aerosols and mixtures of biomass-burning aerosols and dust by means of multi-wavelength depolarization and Raman lidar measurements during SAMUM 2. *Tellus B*, 63: 706–724. doi:10.1111/j.1600-0889.2011.00556, 2011.
- Groß, S., Gasteiger, J., Freudenthaler, V., Müller, T., Sauer, D., Toledano, C., and Ansmann, A.: Saharan dust contribution to the Caribbean summertime boundary layer – a lidar study during SALTRACE, *Atmos. Chem. Phys.*, 16, 11535-11546, doi:10.5194/acp-16-11535-2016, 2016.
- Groot Zwaaftink, C. D., Grythe H., Skov H., and Stohl A.: Substantial contribution of northern high-latitude sources to mineral dust in the Arctic, *J. Geophys. Res. Atmos.*, 121, 13,678–13,697, doi:10.1002/2016JD025482, 2016.

- Guirado, C., Cuevas, E., Cachorro, V. E., Toledano, C., Alonso-Pérez, S., Bustos, J. J., Basart, S., Romero, P. M., Camino, C., Mimouni, M., Zeudmi, L., Goloub, P., Baldasano, J. M., and de Frutos, A. M.: Aerosol characterization at the Saharan AERONET site Tamanrasset. *Atmos. Chem. Phys.* 14(21), 11753-11773. doi:10.5194/acp-14-11753-2014, 2014.
- Haywood, J., Pelon, J., Formenti, P., et al.: Overview of the dust and biomass burning experiment and African monsoon multidisciplinary analysis special observing period-0, *J. Geophys. Res.*, 113, D00C11, doi:10.1029/2008JD010077, 2008.
- Highwood, E. and Ryder, C. (2014) Radiative effects of dust. In: Knippertz, P. and Stuut, J.-B. W. (eds.) *Mineral Dust A Key Player in the Earth System*. Springer, USA, pp. 267-286. ISBN 9789401789776
- Holben, B. N., Eck, S., Slutsker, I., Tanré, D., Buis, J. P., Setzer, A., Vermote, E., and Smirnov, A.: AERONET - A federated instrument network and data archive for aerosol characterization. *Remote. Sens. Environ.* 66(1), 1-16. doi: 10.1016/S0034-4257(98)00031-5, 1998.
- Horowitz, H. M., Garland, R. M., Thatcher, M., Landman, W. A., Dedekind, Z., van der Merwe, J., and Engelbrecht, F. A.: Understanding the seasonality and climatology of aerosols in Africa through evaluation of CCAM aerosol simulations against AERONET measurements, *Atmos. Chem. Phys. Discuss.*, <https://doi.org/10.5194/acp-2017-250>, in review, 2017.
- Huneus, N., Schulz, M., Balkanski, Y., Griesfeller, J., Prospero, J., Kinne, S., Bauer, S., Boucher, O., Chin, M., Dentener, F., Diehl, T., Easter, R., Fillmore, D., Ghan, S., Ginoux, P., Grini, A., Horowitz, L., Koch, D., Krol, M. C., Landing, W., Liu, X., Mahowald, N., Miller, R., Morcrette, J.-J., Myhre, G., Penner, J., Perlwitz, J., Stier, P., Takemura, T., and Zender, C. S.: Global dust model intercomparison in AeroCom phase I, *Atmos. Chem. Phys.*, 11, 7781-7816, doi:10.5194/acp-11-7781-2011, 2011.
- Jickells, T.D., An, Z. S., Andersen, K. K., Baker, A. R., Bergametti, C., Brooks, N., and Cao, J. J., Boyd, P., W. Duce, R. A., Hunter, K. A., Kawahata, H., Kubilay, N., LaRoche, J., Liss, P. S., Mahowald, N., Prospero, J. M., Ridgwell, A. J., Tegen, I., and Torres, R.: Global Iron Connections Between Desert Dust, Ocean Biogeochemistry, and Climate. *Science* 308, 67-71, doi: 10.1126/science.1105959, 2005.
- Kalnay, E., Kanamitsu, M., Kistler, R., Collins, W., Deaven, D., Gandin, L., Iredell, M., Saha, S., White, G., Woollen, J., Zhu, Y., Chelliah, M., Ebisuzaki, W., Higgins, W., Janowiak, J., Mo, K.C., Ropelewski, C., Wang, J., Leetmaa, A., Reynolds, R., Jenne, R., and Joseph, D.: The NCEP/NCAR 40-year reanalysis project, *Bull. Amer. Meteor. Soc.*, 77, 437-470, 1996.
- Karydis, V. A., A. P. Tsimpidi, S. Bacer, A. Pozzer, A. Nenes, J. Lelieveld (2017): Global impact of mineral dust on cloud droplet number concentration. *Atmos. Chem. Phys.* 17(9), 5601-5621. doi: 10.5194/acp-17-5601-2017.
- Kaufman, Y. J., Koren, I., Remer, L. A., Tanré, D., Ginoux, P., and Fan, S.: Dust transport and deposition observed from the Terra-Moderate Resolution Imaging Spectroradiometer (MODIS) spacecraft over the Atlantic Ocean, *J. Geophys. Res.*, 110, D10S12, doi:10.1029/2003JD004436, 2005.
- Knippertz, P., Stuut, J.-B.W. Chapter 1 Introduction. In: Knippertz, P., Stuut, J.-B.W. (Eds.), *Mineral Dust: A Key Player in the Earth System*. Springer, New York, pp. 1–14. <http://dx.doi.org/10.1007/978-94-017-8978-3>, 2014.

- Kim, D., Chin, M., Yu, H., Eck, T. F., Sinyuk, A., Smirnov, A., and Holben, B. N.: Dust optical properties over North Africa and Arabian Peninsula derived from the AERONET dataset. *Atmos. Chem. Phys.* 11, 10733–10741. <http://dx.doi.org/10.5194/acp-11-10733-2011>, 2011.
- Leon, J. F., Derimian, Y., Chiapello, I., Tanre, D., Podvin, T., Chatenet, B., Diallo, A., and Deroo, C.: Aerosol vertical distribution and optical properties over M'Bour (16.96 degrees W; 14.39 degrees N), Senegal from 2006 to 2008, *Atmos Chem Phys*, 9, 9249-9261, 10.5194/acp-9-9249-2009, 2009.
- Mallet, M., Dubovik, O., Nabat, P., Dulac, F., Kahn, R., Sciare, J., Paronis, D., and Léon, J.F.: Absorption properties of Mediterranean aerosols obtained from multi-year ground-based remote sensing observations. *Atmos. Chem. Phys.*, 13 (18), 9195-9210, 2013.
- 10 Martet, M., Peuch, V.H., Laurent, B., and Marticorena, B.: Evaluation of long-range transport and deposition of desert dust with the CTM MOCAGE, *Tellus 61B*, 446-463. DOI: 10.1111/j.1600-0889.2008.00413.x, 2009.
- Maring, H., D. L. Savoie, M. A. Izaguirre, L. Custals, and J. S. Reid: Mineral dust aerosol size distribution change during atmospheric transport, *J. Geophys. Res.*, 108(D19), 8592, doi:10.1029/2002JD002536, 2003.
- Mateos, D., Antón, M., Toledano, C., Cachorro, V. E., Alados-Arboledas, L., Sorribas, M., and Baldasano, J. M.: Aerosol radiative effects in the ultraviolet, visible, and near-infrared spectral ranges using long-term aerosol data series over the Iberian Peninsula. *Atmos. Chem. Phys.* 14(24), 13497-13514. doi:10.5194/acp-14-13497-2014, 2014.
- Meloni, D., di Sarra, A., Pace, G., and Monteleone, F.: Optical properties of aerosols over the central Mediterranean. 2. Determination of single scattering albedo at two wavelengths for different aerosol types. *Atmos. Chem. Phys.* 6, 715-727, 2006.
- 20 Prats, N., Cachorro, V. E., Berjón, A., Toledano, C., and De Frutos, A. M.: Column-integrated aerosol microphysical properties from AERONET Sun photometer over southwestern Spain, *Atmos. Chem. Phys.*, 11, 12535-12547, doi:10.5194/acp-11-12535-2011, 2011. Prospero, J.M., Glaccum, R.A., and Nees, R.T.: Atmospheric transport of soil dust from Africa to South America, *Nature* 289 (5798), 570-572, 1981.
- Prospero, J. M., and Peter J. L.: African Droughts and Dust Transport to the Caribbean: Climate Change Implications. *Science* 302 (5647):1024-1027. doi: 10.1126/science.1089915, 2003.
- Prospero, J. M., and Mayol-Bracero O. L.: Understanding the transport and impact of African dust on the Caribbean Basin. *Bulletin of the American Meteorological Society* 94 (9):1329-1337. doi: 10.1175/BAMS-D-12-00142.1, 2013.
- Prospero, J.M., Glaccum, R.A., and Nees, R.T.: Atmospheric transport of soil dust from Africa to South America, *Nature* 289 (5798), 570-572, 1981.
- 30 Prospero, J. M.: Long-term measurements of the transport of African mineral dust to the southeastern United States: Implications for regional air quality, *J. Geophys. Res.-Atmos.*, 104(D13), 15917–15927, 1999.
- Prospero, J.M., Blades, E., Mathison, G., and Naidu, R.: Interhemispheric transport of viable fungi and bacteria from Africa to the Caribbean with soil dust, *Aerobiologia* 21, 1-19, DOI 10.1007/s10453-004-5872-7, 2005

- Prospero, J. M., Collard, F.X., Molinié, J., and Jeannot, A. Characterizing the annual cycle of African dust transport to the Caribbean Basin and South America and its impact on the environment and air quality. *Global Biogeochemical Cycles*:2013GB004802. doi: 10.1002/2013GB004802, 2014.
- Reid, J.S., Kinney, J.E., Westphal, D.L., Holben, B.N., Welton, E.J., Tsay, S.-., Eleuterio, D.P., Campbell, J.R., Christopher,
5 S.A., Colarco, P.R., Jonsson, H.H., Livingston, J.M., Maring, H.B., Meier, M.L., Pilewskie, P., Prospero, J.M., Reid, E.A., Remer, L.A., Russell, P.B., Savoie, D.L., Smirnov, A. and Tanré, D.: Analysis of measurements of Saharan dust by airborne and ground-based remote sensing methods during the Puerto Rico Dust Experiment (PRIDE), *J. Geophys. Res.*, 108(D19), 8586, doi:10.1029/2002JD002493, 2003.
- Rodríguez, S., Cuevas, E., Prospero, J. M., Alastuey, A., Querol, X., López-Solano, J., García, M. I., and Alonso-Pérez, S.:
10 Modulation of Saharan dust export by the North African dipole, *Atmos. Chem. Phys.*, 15, 7471-7486, <https://doi.org/10.5194/acp-15-7471-2015>, 2015.
- Savoie, D. L., Arimoto, R., Keene, W. C., Prospero, J. M., Duce, R. A. and Galloway, J. N.: Marine biogenic and anthropogenic contributions to non-sea-salt sulfate in the marine boundary layer over the North Atlantic Ocean. *Journal of Geophysical Research: Atmospheres* 107 (D18):4356. doi: 10.1029/2001JD000970, 2002.
- Smirnov, A., Holben, B. N., Savoie, D., Prospero, J. M., Kaufman, Y. J., Tanre, D., Eck, T. F., and Slutsker, I.: Relationship
15 between column aerosol optical thickness and in situ ground based dust concentrations over Barbados. *Geophysical Research Letters* 27 (11):1643-1646, 2000.
- Stein, A.F., Draxler, R.R., Rolph, G.D., Stunder, B.J.B., Cohen, M.D., and Ngan, F.: NOAA's HYSPLIT atmospheric transport and dispersion modeling system, *Bull. Amer. Meteor. Soc.*, 96, 2059-2077, 2015.
- Tegen, I., Schepanski, K., and Heinold, B.: Comparing two years of Saharan dust source activation obtained by regional
20 modelling and satellite observations, *Atmos Chem Phys*, 13, 2381-2390, 10.5194/acp-13-2381-2013, 2013.
- Toledano, C., Wiegner, M., Groß, S., Freudenthaler, V., Gasteiger, J., Müller, D., Müller, T., Schladitz, A., Weinzierl, B., Torres, B., and O'Neill, N. T.: Optical properties of aerosol mixtures derived from sun-sky radiometry during SAMUM-2. *Tellus B.* 63, 635–648, 2011.
- Valenzuela, A., Olmo, F. J., Lyamani, H., Antón, M., Quirantes, A., and Alados-Arboledas, L.: Aerosol radiative forcing
25 during African desert dust events (2005–2010) over Southeastern Spain. *Atmos. Chem. Phys.* 12(21), 10331–10351, doi:10.5194/acp-12-10331-2012, 2012.
- Valle-Díaz, C.J., Torres-Delgado E., Colón-Santos S.M., Lee T., Collett Jr J.L., McDowell W.H., and Mayol-Bracero O.L.:
Impact of long-range transported African dust on cloud water chemistry at a tropical montane cloud forest in northeastern
30 Puerto Rico. *Aerosol and Air Quality Research* 16: 653–664, DOI: 10.4209/aaqr.2015.05.0320, 2016.
- Weinzierl, B., Ansmann, A., Prospero, J.M., Althausen, D., Benker, N., Chouza, F., Dollner, M., Farrell, D., Fomba, W.K., Freudenthaler, V., Gasteiger, J., Groß, S., Haario, M., Heinold, B., Kandler, K., Kristensen, T.B., Mayol-Bracero, O.L., Müller, T., Reitebuch, O., Sauer, D., Schäfler, A., Schepanski, K., Spanu, A., Tegen, I., Toledano, C. and Walser, A.: The

- Saharan aerosol long-range transport and aerosol-cloud-interaction experiment: Overview and selected highlights. *Bulletin of the American Meteorological Society*, vol. 98, no. 7, pp. 1427-1451, 2017,
- Yu, H., Chin M., Bian H., Yuan T., Prospero J. M., Omar A. H., Remer L. A., Winker D. M., Yang Y., Zhang Y., and Zhang Z.: Quantification of trans-Atlantic dust transport from seven-year (2007-2013) record of CALIPSO lidar measurements. *Remote Sensing of Environment* 159:232-249. doi: 10.1016/j.rse.2014.12.010, 2014.
- 5 Yu, H., Chin, M., Yuan, T., Bian, H., Remer, L.A., Prospero, J.M., Omar, A., Winker, D., Yang, Y., Zhang, Y., Zhang, Z. and Zhao, C.: The fertilizing role of African dust in the Amazon rainforest: A first multiyear assessment based on data from Cloud-Aerosol Lidar and Infrared Pathfinder Satellite Observations. *Geophysical Research Letters*: 2015GL063040. doi: 10.1002/2015GL063040, 2015.
- 10 Zamora, L. M., Prospero, J. M., Hansell, D. A., and Trapp, J. M.: Atmospheric P deposition to the subtropical North Atlantic: sources, properties, and relationship to N deposition. *Journal of Geophysical Research: Atmospheres* 118 (3):1546-1562. doi: 10.1002/jgrd.50187, 2013.

Table 1. Geographical coordinates, considered time period and total number of level 2.0 AOD daily data from the different AERONET sites used for the global African and Caribbean databases. To highlight the number of available inversion products, the number of daily data of volume particle size distribution (VPSD) is presented.

5

Area	Site	Coordinates (°N, °E, m a.s.l.)	Time period	Number of AOD / VPSD daily data
AF	Capo_Verde (CV)	(16.71, -22.93, 60)	1993-2014	4635/1910
	Dakar (DK)	(14.38, -16.95, 0)	1996-2014	3593/2466
CAR	Barbados (BA)	(13.15, -59.62, 114)	1996-2000	938/50
	Barbados_SALTRACE (BA)		2013-2014	181/7
	Ragged_Point (RG)	(13.15, -59.42, 40)	2007-2014	1768/415
	Guadeloup (GU)	(16.22, -61.53, 39)	1997-2014	1949/441
	La_Parguera (LP)	(17.97, -67.03, 12)	2000-2014	3303/1467
	Cape_San_Juan (SJ)	(18.38, -65.62, 15)	2004-2014	1901/401

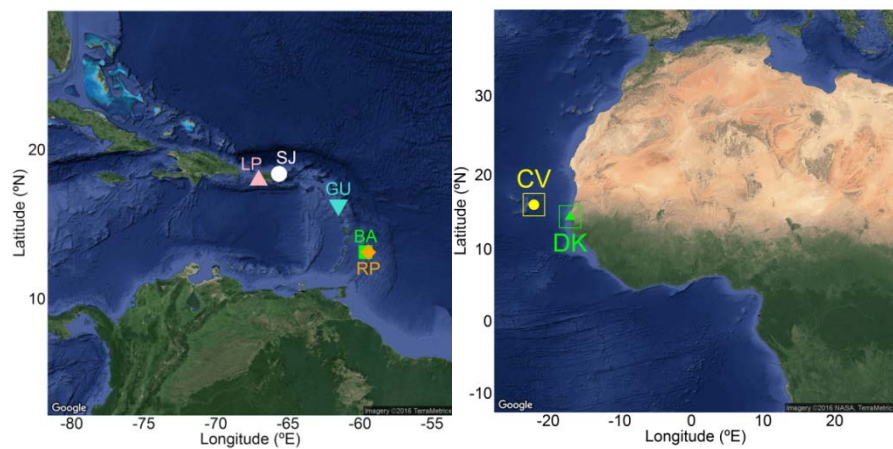


Figure 1: AERONET sites in the Caribbean Zone (left) and African zone (right). For acronyms see Table 1.

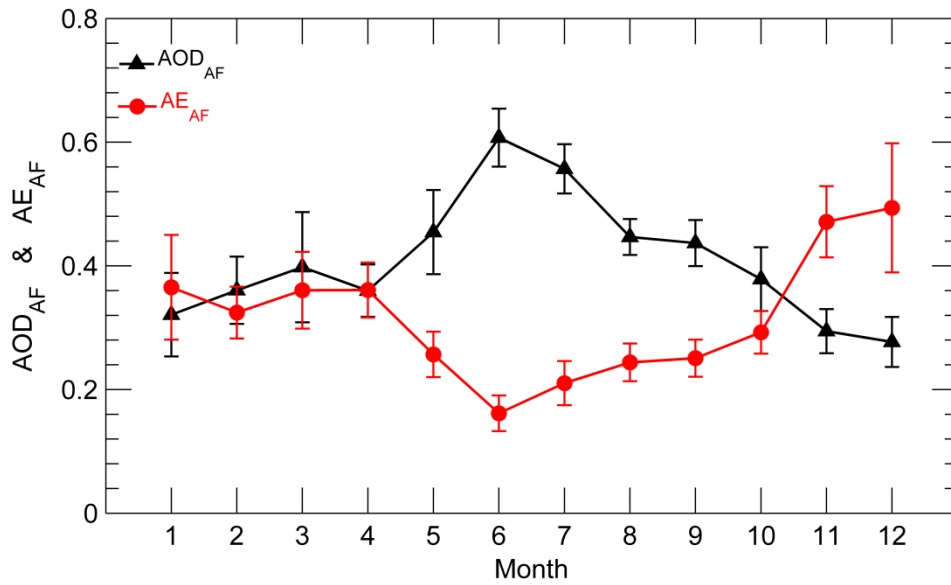


Figure 2: Monthly average of AOD and AE from 1996 to 2014 in the African area. The number of daily means used in the multi-annual averages is 5656.

5

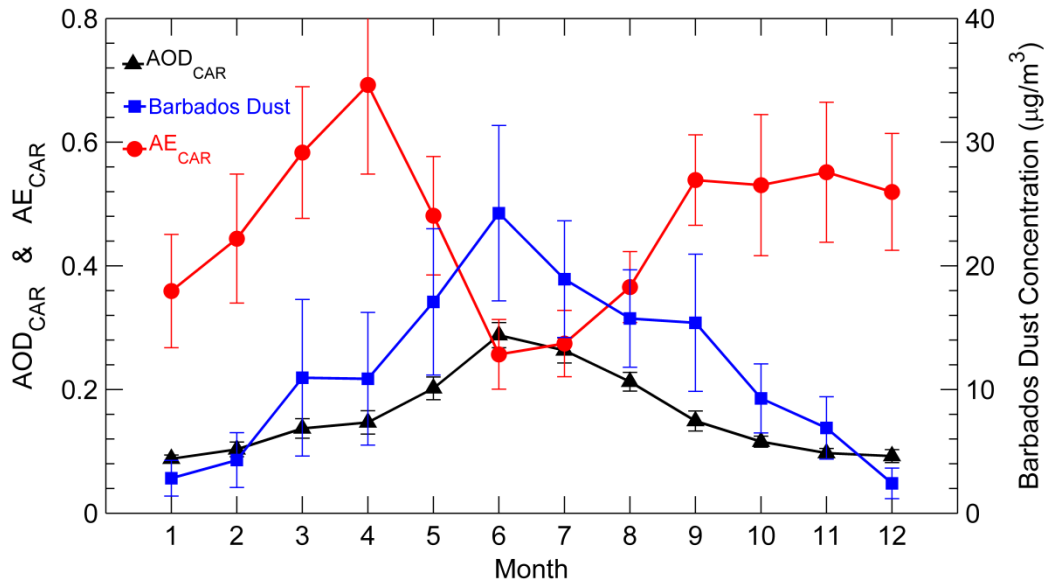


Figure 3. Monthly average of AOD and AE in the Caribbean area from 1996 to 2014 and surface dust concentrations in Barbados in the period 1996-2011. The number of daily means used in the multi-annual averages is 5099 for AODCAR and AECAR and 5167 for surface dust concentration in Barbados.

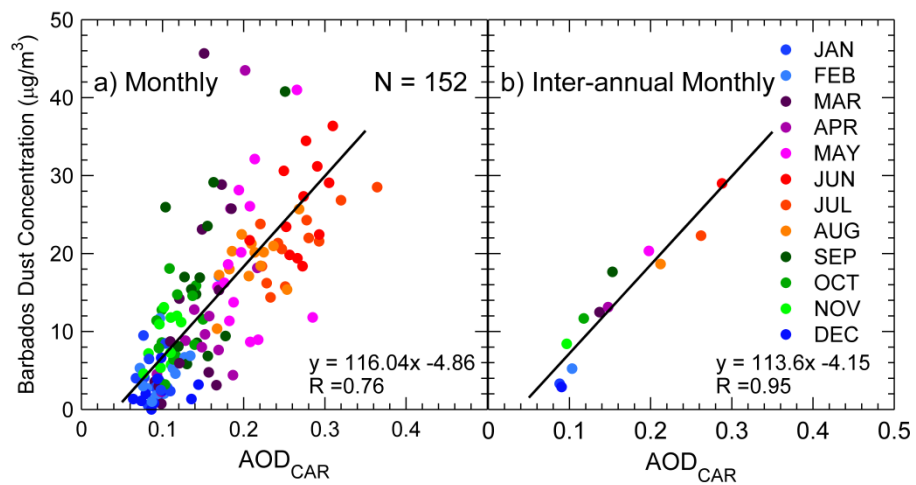


Figure 4: Scatterplot of: (a) monthly and (b) inter-annual monthly means of surface dust concentration and AOD in the Caribbean Basin in the period 1996-2011. Solid line highlights the linear fit between both quantities.

5

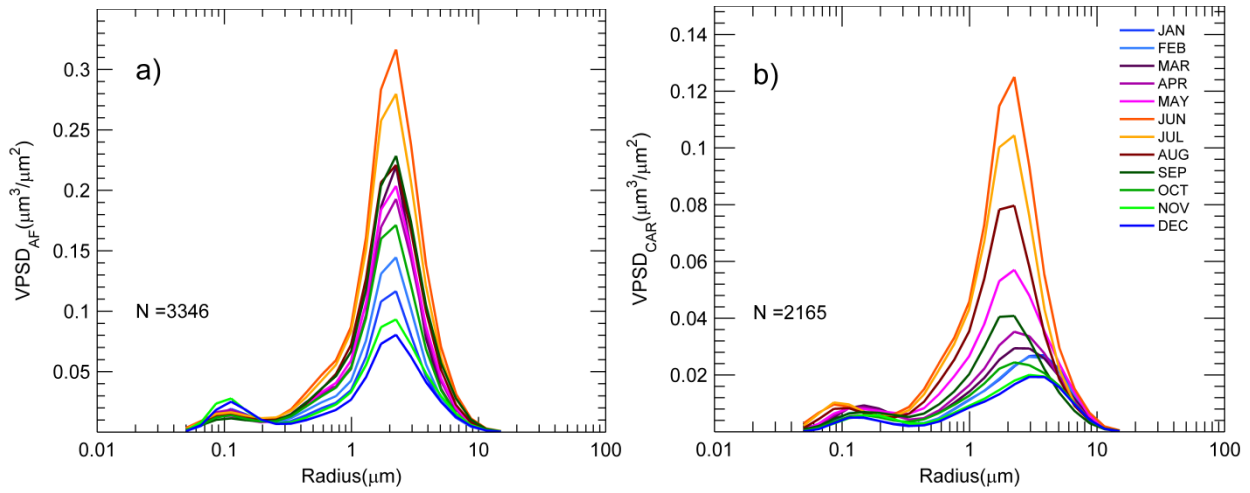


Figure 5: Monthly averages of VPSD from 1996 to 2014 in West African (a) and Caribbean (b) areas.

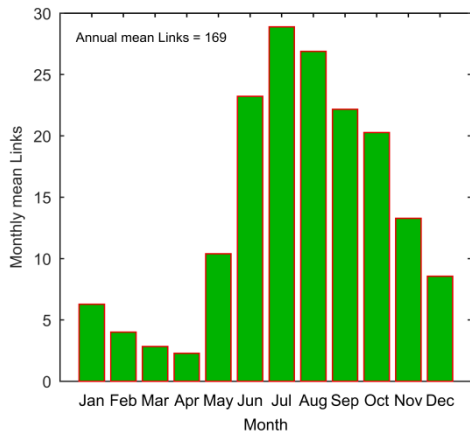
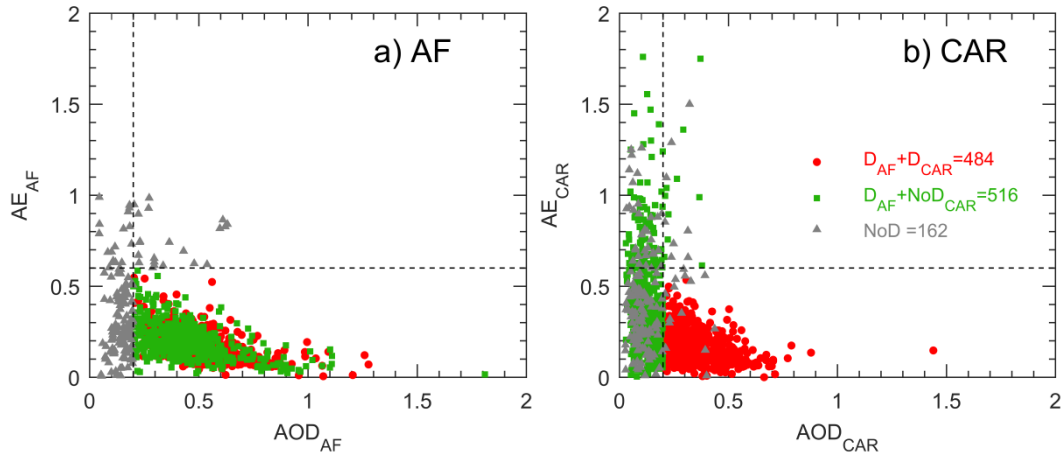


Figure 6. Seasonal cycle of number of Africa-Caribbean Sea air mass connections. The total number of air mass links is 169 per year, with a total of 3174 links in the 19-year analyzed period.

5



5

Figure 7: AE-AOD scatterplot for all data days in a) West Africa and b) Caribbean Sea. Red circles are dust days in both Africa (D_{AF}) and Caribbean (D_{CAR}) databases, green squares are dust days in Africa which are not dusty in Caribbean area (NoD_{CAR}), and grey triangles are non-dusty days (“NoD”) in both areas. Dashed lines indicate the criteria for identifying mineral dust ($AOD \geq 0.2$ and $AE \leq 0.6$).

10

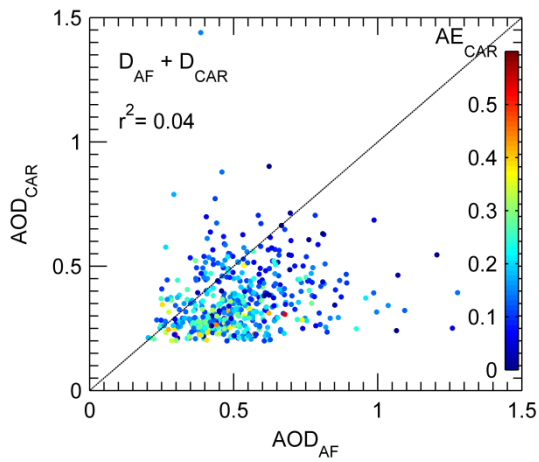


Figure 8. Scatterplot of AOD in the Caribbean (AOD_{CAR}) versus AOD in the African zone (AOD_{AF}). The color bar indicates the AE in the Caribbean zone (AE_{CAR}) when dust is observed in both areas ($D_{AF}+D_{CAR}$ case, see Section 5 2.2). Solid lines point out no change in AOD data between both areas.

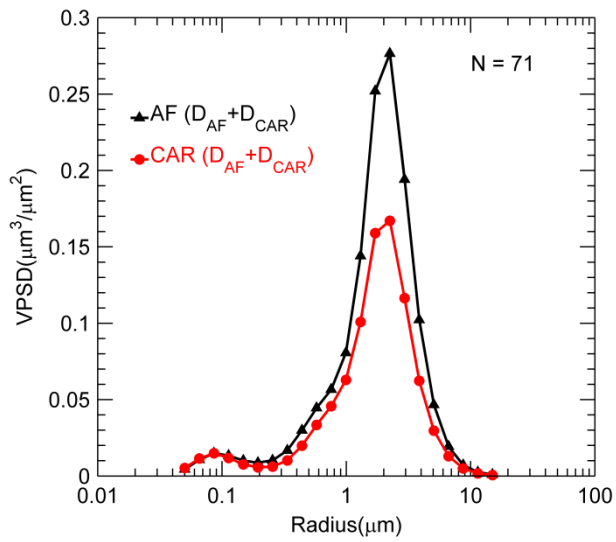


Figure 9: VPSD in the African (AF) and the Caribbean (CAR) areas under desert dust conditions (“ $D_{AF} + D_{CAR}$ ” case, see Section 2.2).

5

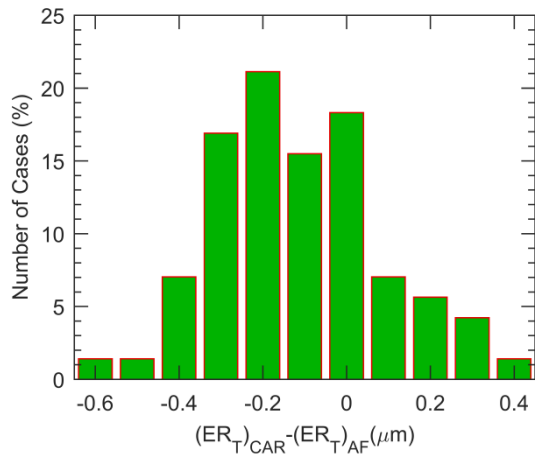


Figure 10: Histogram of the differences between the total effective radii in the African zone and in the Caribbean area for those cases with connected desert dust conditions in both areas (“ $D_{AF} + D_{CAR}$ ” case).

5

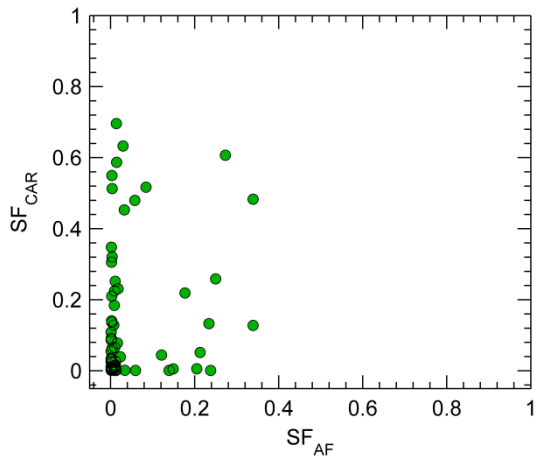


Figure 11: Sphericity fraction values in the African zone and in the Caribbean area for those cases with desert dust in both areas.

5

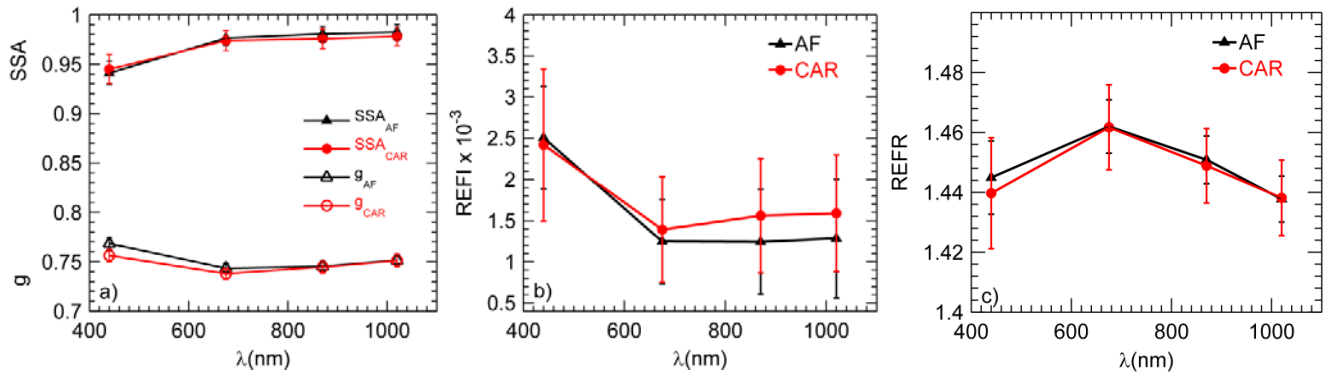


Figure 12: a) Single scattering albedo (SSA) and asymmetry parameter (g), b) Imaginary part of the refractive index (REFI), c) Real part of the refractive index (REFR) for those cases with desert dust in both African zone (black lines)

5 and Caribbean area (red lines).